Text S1. X-ray micro-computed tomography

Micro-XCT was performed on 22 NPS samples using a Nikon XT-H-225-XCT Scanner. Original processed images were downsampled to 30μm voxel resolution to reduce image size and speed up processing. Surfaces are generated from segmented images in PerGeos 2020.2 using built in algorithm. Surfaces with application of Gaussian smoothing were compared to unsmoothed surfaces and selected for further analysis. All surfaces were edited using Surface Edit tool to remove polygons not pertaining to area of interest and resulting areas calculated as a mean value of opposing fracture sides.

Text S2. Permeability measurements

Single-phase permeability measurements were performed on eight samples of NPS, each at a different fracture orientation. Following testing, two of the samples (Arrester and 60° to bedding) were found to contain signs of confining fluid leakage, and so these two samples were discarded from further analysis.

Sample permeability was measured using the steady state method, with Nitrogen as the permeating fluid, and all tests were carried out at 25°C. Experiments at each pressure step were continued until a constant flow rate was reached, thus satisfying the steady-state test requirements.

Two loading and unloading cycles were carried out for each sample, where a significant amount of hysteresis is observed between the first loading cycle and the subsequent cycles. This is common in such experiments (Cuss *et al.* 2017; Houben *et al.* 2020), and is due to the sample being loaded from ambient pressure conditions in the first cycle. As our analysis is focused on fluid flow in the subsurface, we omit this first loading cycle from our analysis, and a mean permeability at each effective stress state is calculated from the first unloading cycle, and the subsequent loading and unloading cycle.

A list of testing conditions and results are provided in Table S1, and an illustration of a full dataset for the Divider sample is provided in figure S1.

Table S1: Testing conditions are permeability data for each of the samples used for this study.

Fracture Orientation	**Mean Effective Stress (MPa)**	**Permeability (m^2)**
Short-transverse	20.26	1.87E-16

Short-transverse	14.39	1.95E-16
Short-transverse	8.28	2.07E-16
Short-transverse	2.17	5.84E-16
15°	20.21	3.61E-16
15°	14.16	3.75E-16
15°	8.16	4.03E-16
15°	2.12	7.83E-16
30°	20.17	7.86E-17
30°	14.19	8.19E-17
30°	8.32	8.89E-17
30°	2.19	1.52E-16
45°	19.94	4.27E-17
45°	14.10	4.42E-17
45°	8.65	4.89E-17
45°	2.20	7.95E-17
75°	20.11	2.55E-16
75°	14.17	2.92E-16
75°	8.15	4.08E-16
75°	2.20	1.55E-15
Divider	20.20	1.32E-16
Divider	14.27	1.37E-16
Divider	8.24	1.58E-16
Divider	2.12	2.65E-16

24

25

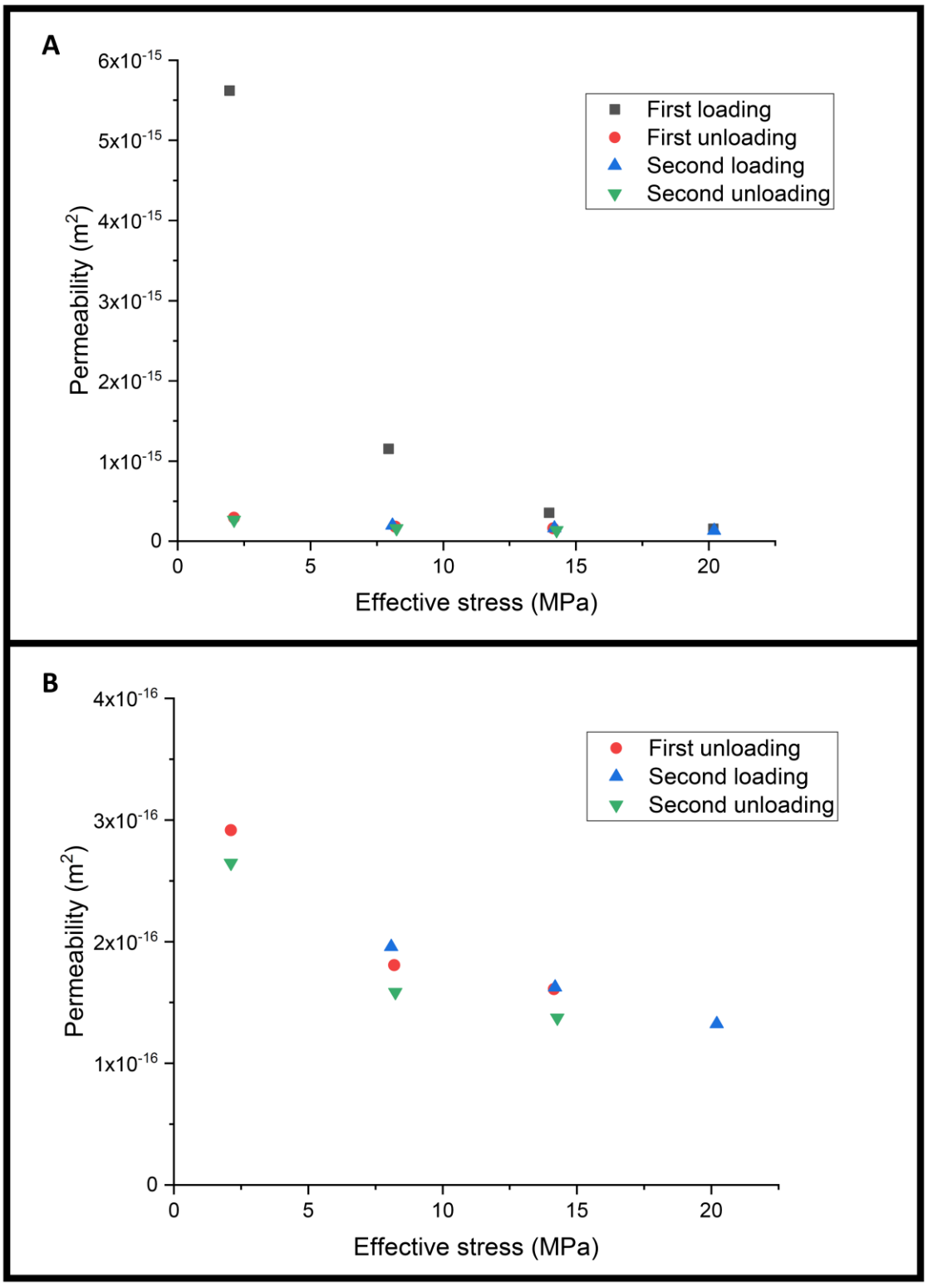

Figure S1: A) Permeability against effective stress data for the Divider sample. B) Permeability against effective stress data for the Divider sample, with the first loading cycle omitted. Note the difference in scale of the Y-axis between A and B.

Text S3. Synchrotron Image Acquisition

X-ray micro-computed tomography imaging was performed using the X02DA TOMCAT beamline at the Swiss Light Source, Paul Scherrer Institute (Villigen, Switzerland). Samples were exposed to filtered (400-µm Aluminium) polychromatic X-ray radiation (energy = 24keV) originating from a 2.9T bending magnet source on a 2.4GeV storage ring (ring current = 401.9mA). X-rays were converted to visible light via a 150µm thick LuAG:Ce scintillator (Crytur, Czech Republic), which were magnified (4x) by a high numerical aperture white-beam microscope (Optique Peter) (Bührer *et al.* 2019) before being recorded by the in-house developed GigaFRoST camera (Mokso *et al.* 2017), which yielded a pixel size of 2.75µm for each tomographic image. Image acquisition details are given in Table S1. Following image acquisition, all 16-bit tomograms were reconstructed from the X-ray projections via absorption-based reconstruction, utilizing the Fourier-based Gridec algorithm (Marone & Stampanoni 2012) with a Parzen filter.

Table S2: Synchrotron image acquisition parameters for each tomographic image shown in Figure 5 of the main text.

No. of scans	1
No. of projections	5000
No. of darks	50
No. of flats	100
Exposure time	0.9ms
Pixel size	2.75µm
Angular rotation range	180°
Rotation velocity	39.82°/s
Original Tiff projection size	2016 x 1480 pixels